Electronic Supplementary Information

A Procedurally Activatable Nanoplatform for Chemo/Chemodynamic Synergistic Therapy

Wen Han,‡[a] Min Wang,‡[a] Huaming He,[a] Yifan Jiang,[a] Chunhua Lu*[a] and Xiankun Tu*[b]

a. Key Laboratory for Analytical Science of Food Safety and Biology of the MOE, Fujian Provincial Key Laboratory of Analysis and Detection Technology for Food Safety, State Key Laboratory of Photocatalysis on Energy and Environment, College of Chemistry, Fuzhou University, Fuzhou 350116, P. R. China.

b. Department of Neurosurgery, Fujian Medical University Union Hospital, Neurosurgical Institute of Fujian Province, Fuzhou, 350001, P.R. China.

E-mail: chunhualu@fzu.edu.cn; unionnstu@hotmail.com

‡ These authors contributed equally to this work.

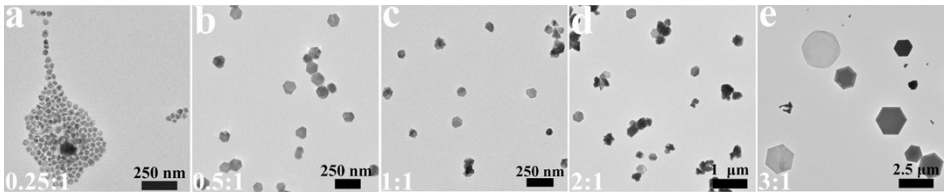

Fig. S1 TEM images of Cu_9S_5 NSs synthesized with $CuCl_2$ / $C_6H_{10}O_4S_2$ molar radios of (a) 0.25:1, (b) 0.5:1, (c) 1:1, (d) 2:1 and (e)3:1.

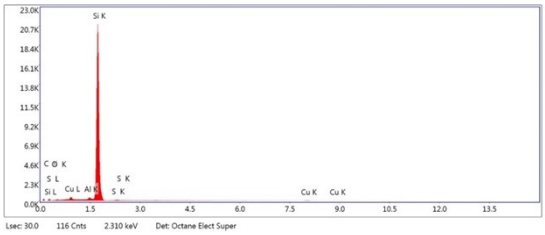

Element	Weight %	Atomic %
C K	67.35	86.53
O K	5.43	5.20
S K	6.83	3.30
CuK	20.39	4.97

Fig. S2 Energy-dispersive X-ray spectroscopy of Cu_9S_5 NSs.

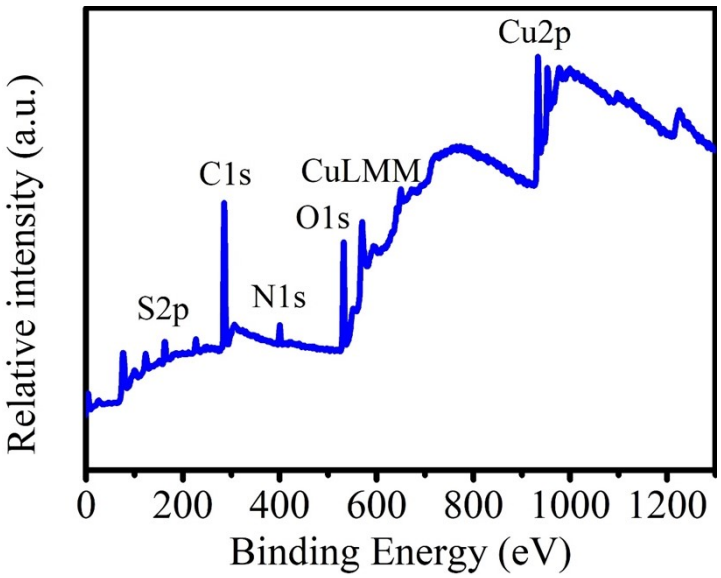

Fig. S3 XPS spectrum of Cu_9S_5 NSs.

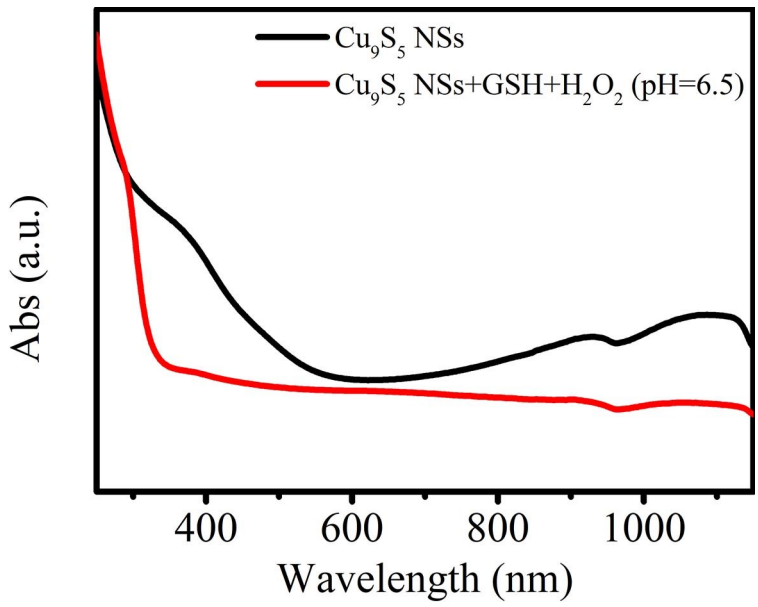

Fig. S4 UV-vis absorption spectra of Cu_9S_5 NSs in the presence or absence of GSH and H_2O_2.

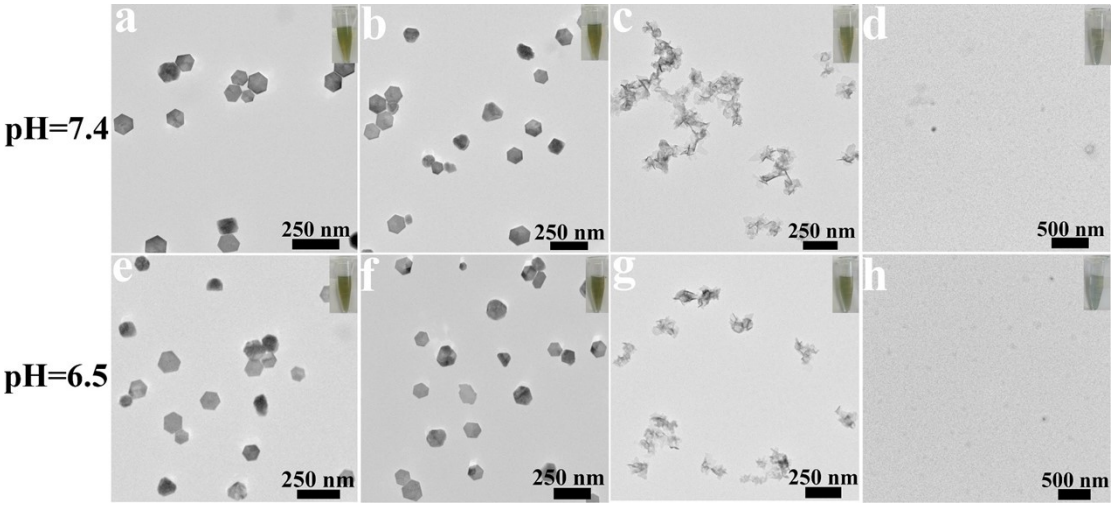

Fig. S5 TEM images of Cu_9S_5 NSs after different treatments for 1 h. (a) control, (b) GSH, (c) H_2O_2, (d) GSH+H_2O_2, (e) control at pH=6.5, (f) GSH, (g) H_2O_2 and (h) GSH + H_2O_2 ([Cu_9S_5 NSs] = 100 μg•mL^{-1}, [GSH] = 1 mM, [H_2O_2] = 10 mM).

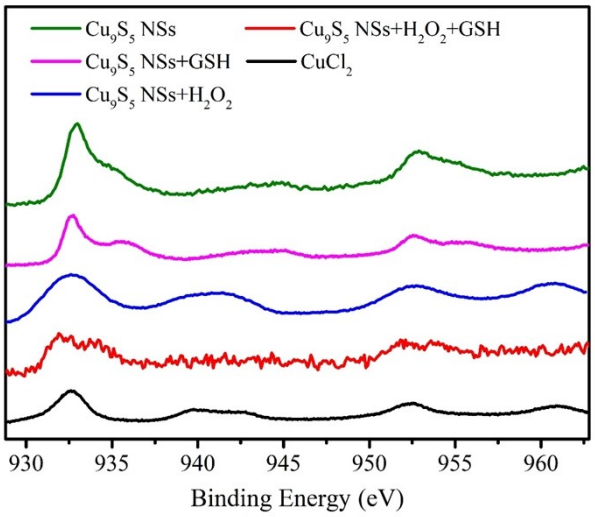

Fig. S6 Cu 2p XPS spectra of Cu_9S_5 NSs, Cu_9S_5 NSs treated with GSH, Cu_9S_5 NSs treated with H_2O_2, Cu_9S_5 NSs treated with H_2O_2/GSH, and $CuCl_2$.

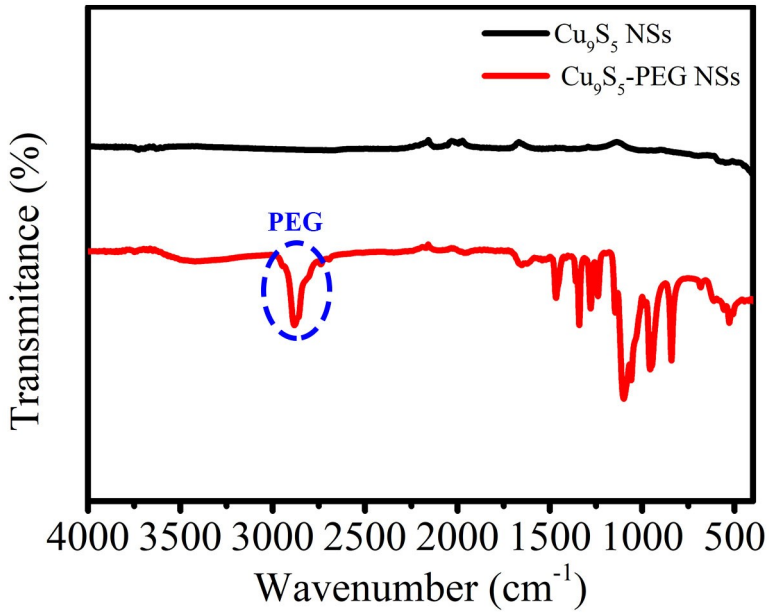

Fig. S7 FTIR spectra of Cu_9S_5 NSs, and Cu_9S_5-PEG NSs.

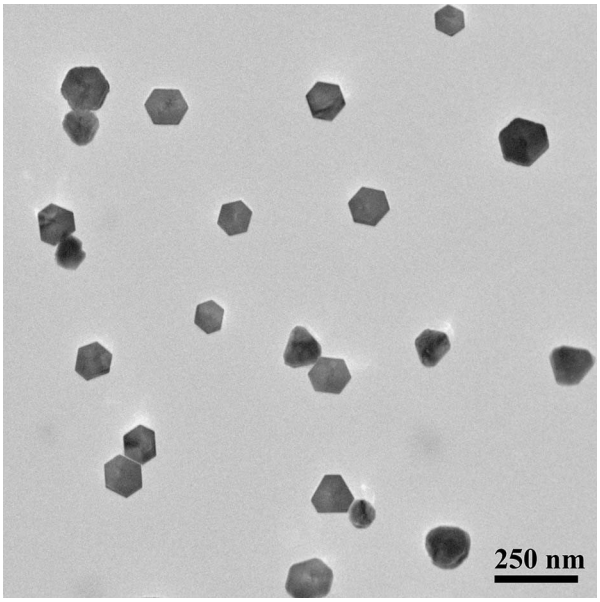

Fig. S8 TEM image of Cu_9S_5-PEG NSs.

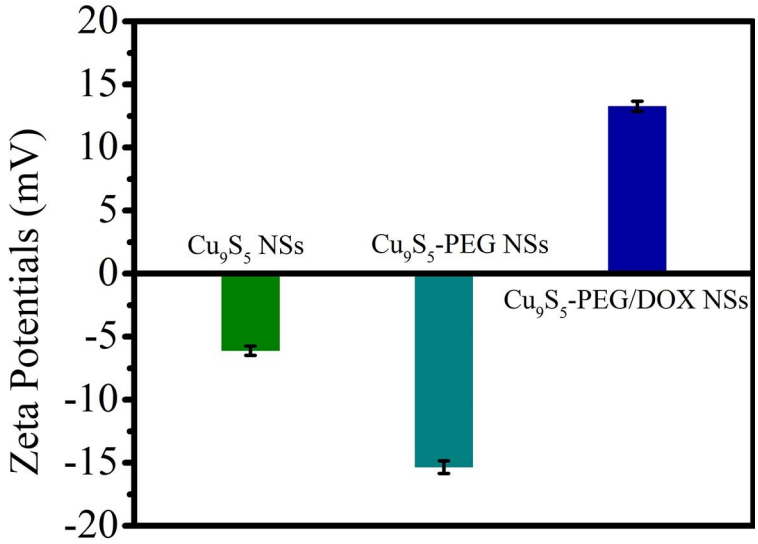

Fig. S9 Zeta potentials of Cu_9S_5 NSs, Cu_9S_5-PEG NSs, and Cu_9S_5-PEG/DOX NSs.

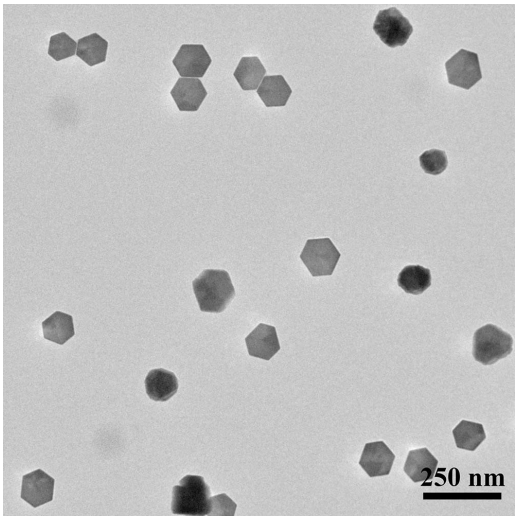

Fig. S10 TEM image of Cu_9S_5-PEG/DOX NSs.

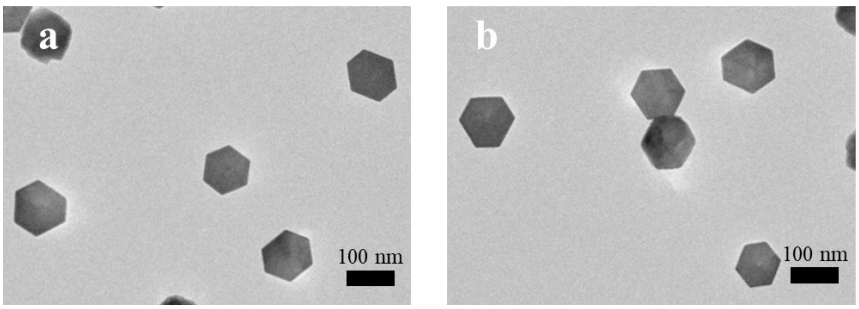

Fig. S11 TEM images of Cu_9S_5-PEG/DOX NSs in different environments: (a)medium and (b) FBS.

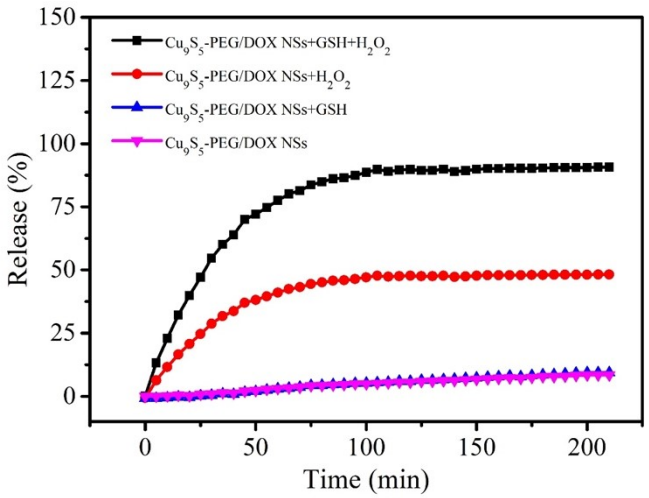

Fig. S12 The DOX releasing rates of Cu_9S_5-PEG/DOX NSs after treatment with different conditions.

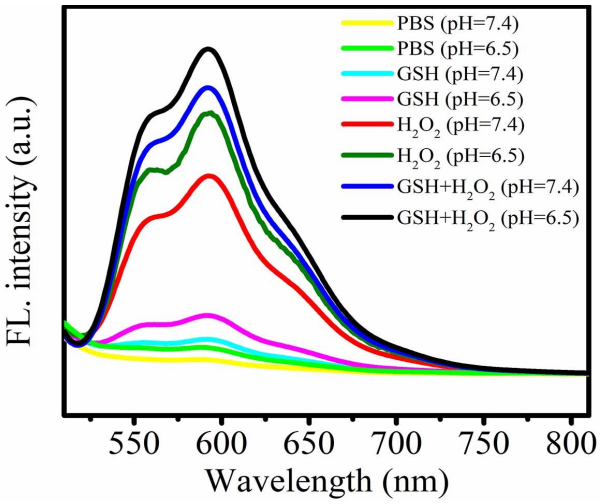

Fig. S13 Fluorescent spectra of Cu_9S_5-PEG/DOX NSs after treatment with different conditions.

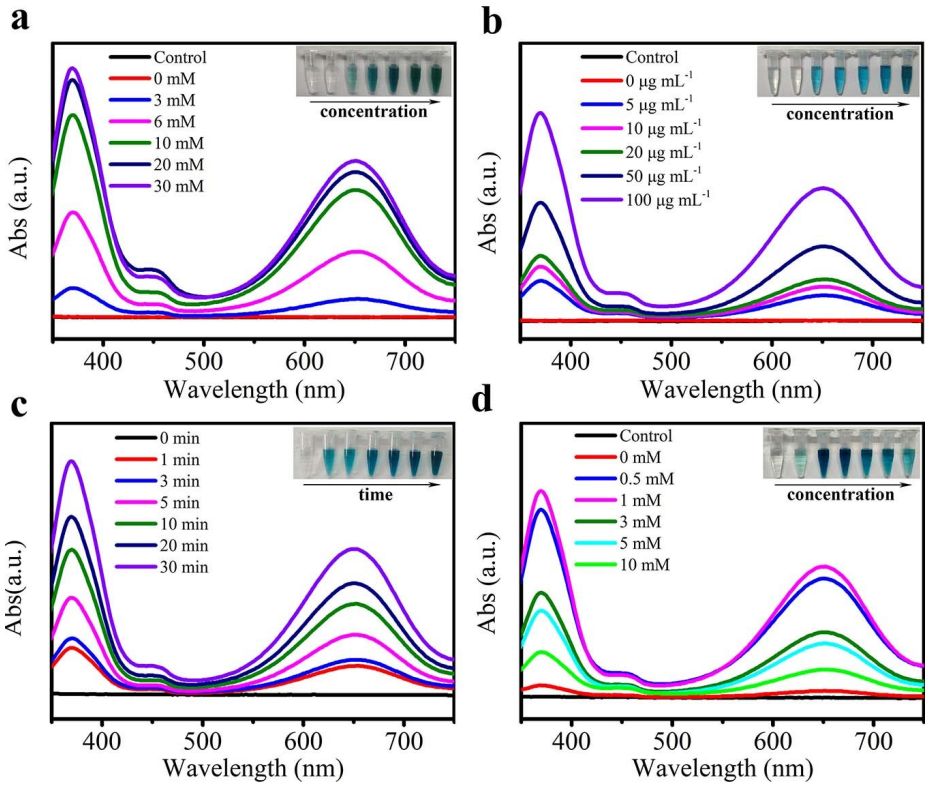

Fig. S14 The UV-vis absorption spectra and visual color changes of TMB aqueous solutions as catalyzed by Cu_9S_5 NSs (a) with GSH (1 mM) at different concentrations of H_2O_2, (b) with GSH (1 mM) and H_2O_2 (10 mM) at different concentrations of Cu_9S_5 NSs, (c) with GSH (1 mM) and H_2O_2 (10 mM) at different reaction times, (d) with H_2O_2 (10 mM) at different concentrations of GSH.

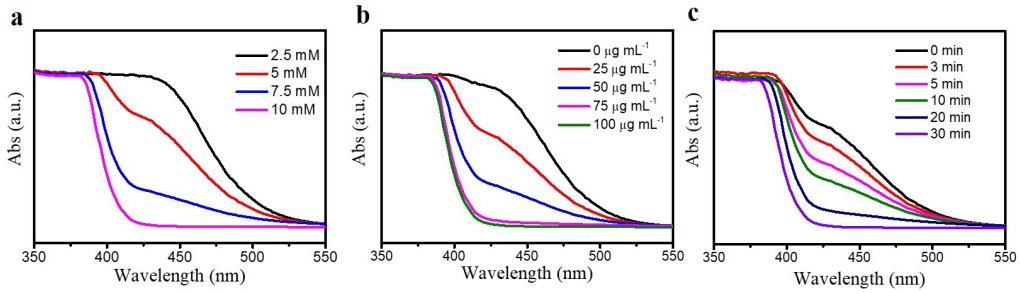

Fig. S15 Decrease of UV-Vis absorption at 410 nm showing the GSH depletion from the redox reaction as catalyzed by Cu_9S_5 NSs (a) with GSH (1 mM) at different concentrations of H_2O_2, (b) with GSH (1 mM) and H_2O_2 (10 mM) at different concentrations of Cu_9S_5 NSs, (c) with GSH (1 mM) and H_2O_2 (10 mM) at different reaction times.

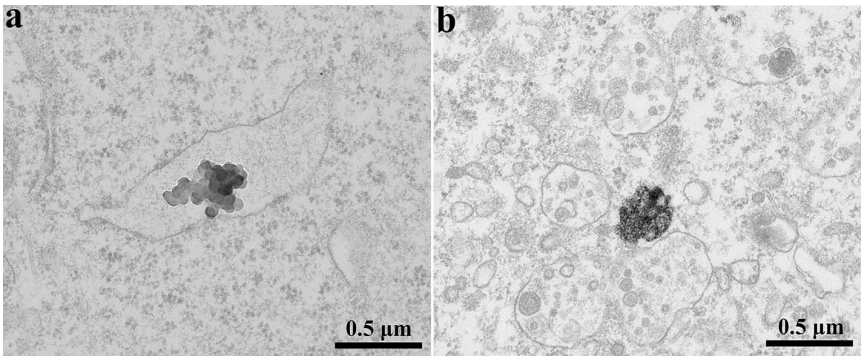

Fig. S16 Bio-TEM images of (a) L02 and (b) MCF-7 cells after incubating with Cu_9S_5-PEG/DOX NSs for 6 h.

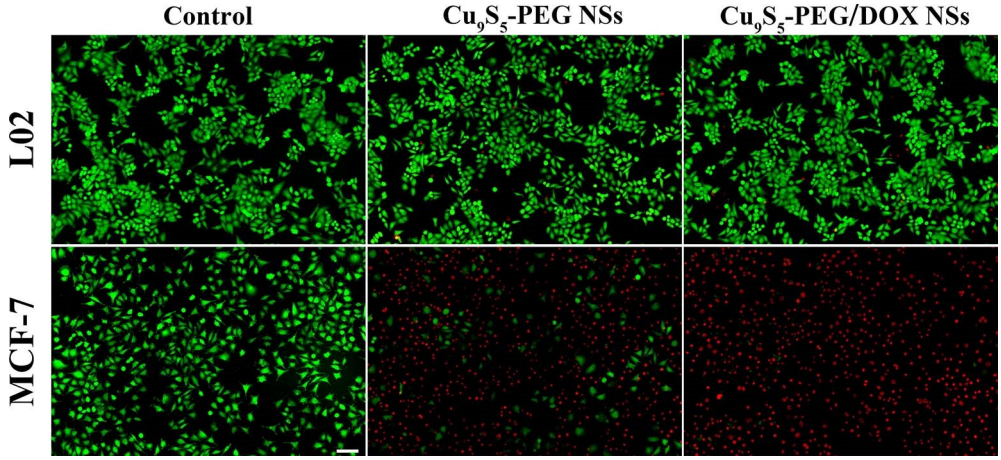

Fig. S17 Live/dead staining of L02 and MCF-7 cells. Green fluorescence shows the live cells stained with calcein AM, and red fluorescence shows the dead cells stained with PI (scale = 100 μm).

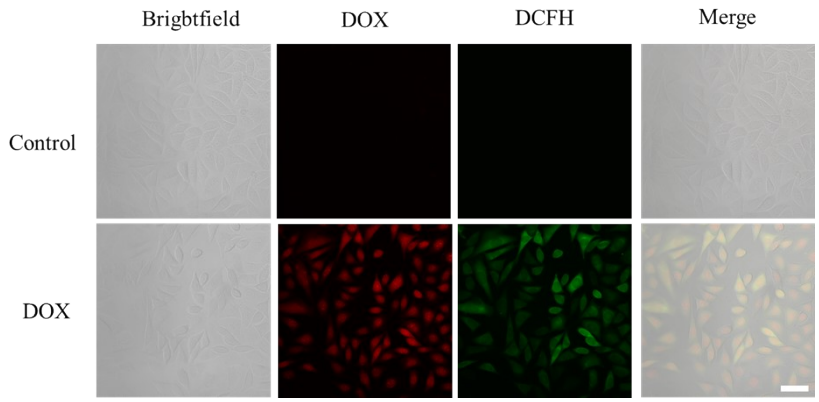

Fig. S18 Confocal fluorescence images of DCFH-DA stained MCF-7 cells after incubation with DOX (scale = 50 μm.)

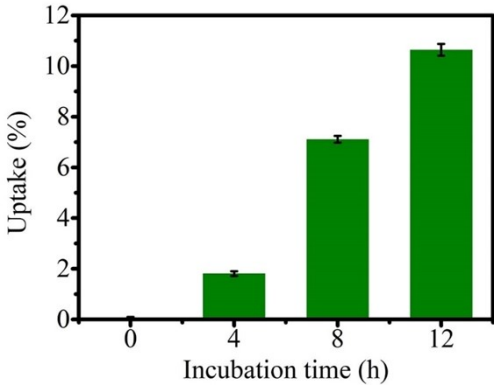

Fig. S19 Intracellular phagocytosis of Cu_9S_5-PEG/DOX NSs after incubating for 0, 4, 8, and 12 h, respectively.

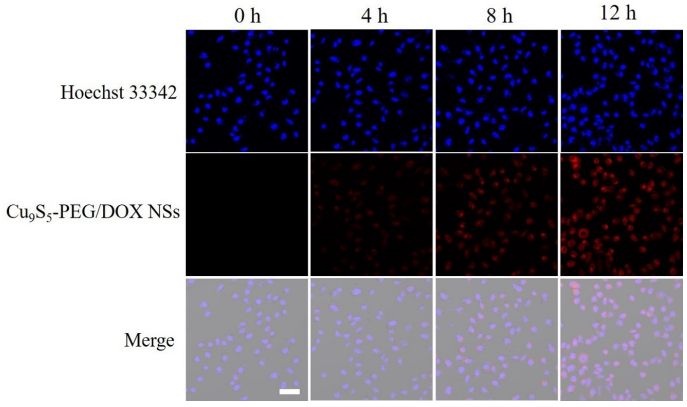

Fig. S20 Confocal fluorescence images of MCF-7 cells treated with Cu_9S_5-PEG/DOX NSs for 0 h, 4 h, 8 h, and 12 h (Scale = 50 μm).

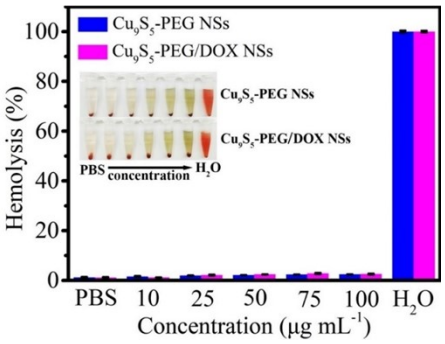

Fig. S21 Relative hemolysis ratios of H_2O, PBS, and different concentrations of Cu_9S_5-PEG NSs and Cu_9S_5-PEG/DOX NSs. The inset was the corresponding photos.

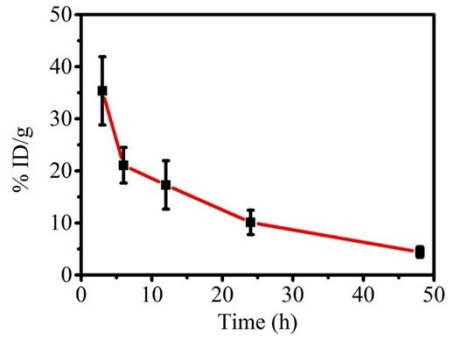

Fig. S22 Blood-circulation curve of intravenously injected Cu_9S_5-PEG/DOX NSs.

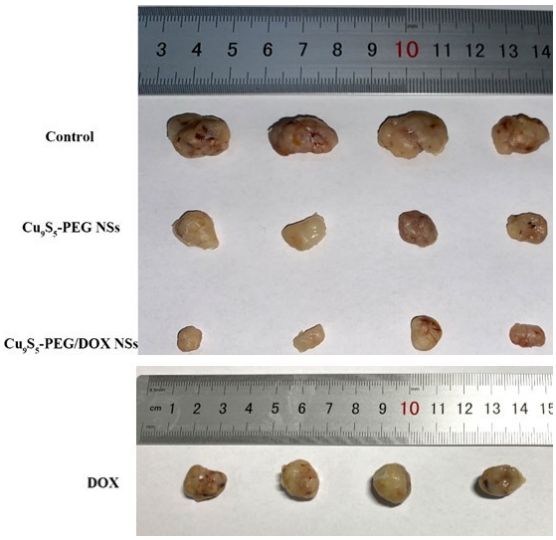

Fig. S23 Visual images of excised tumor treated with PBS (control), DOX, Cu_9S_5-FS NSs, and Cu_9S_5-PEG/DOX NSs on the 14th day.

The tumor inhibition rates of DOX, Cu_9S_5-PEG NSs and Cu_9S_5-PEG/DOX NSs calculated by Fig. 4c were 30.84, 55.52 and 85.52 %, respectively. The synergistic treatment improved outcomes by nearly 30%.

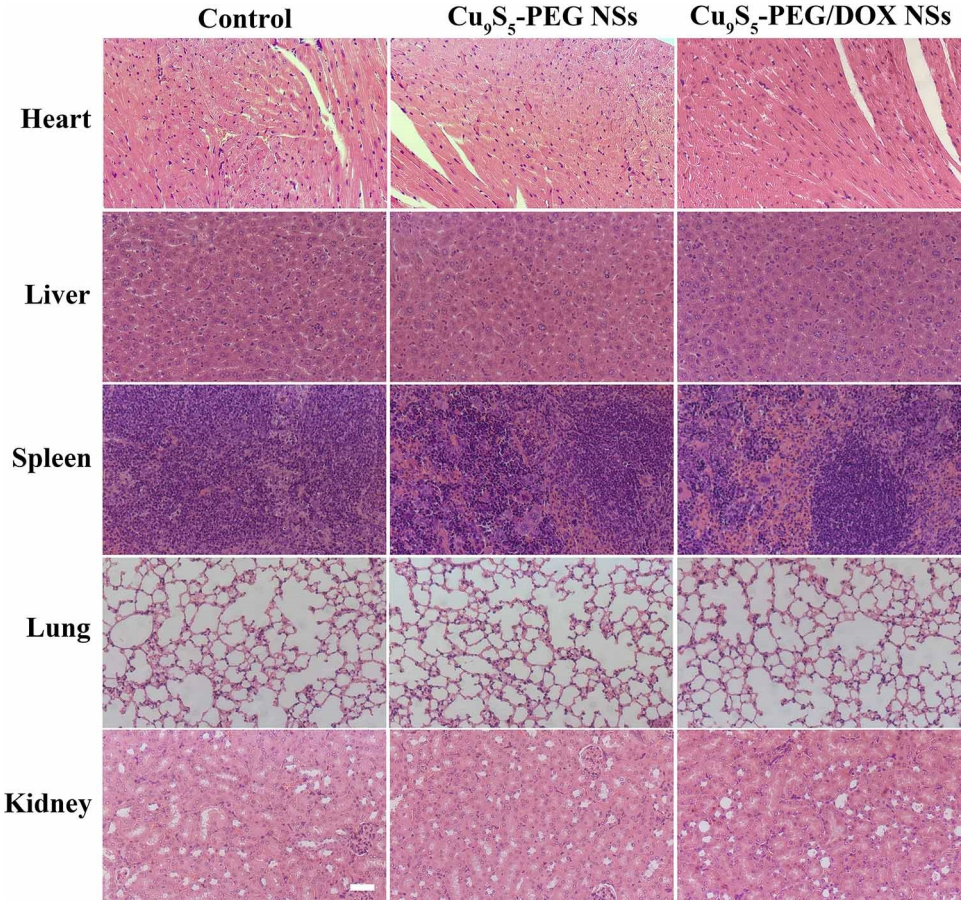

Fig. S24 H&E-stained tissue slices from major organs (heart, liver, spleen, lung, and kidney) of different groups (Scale = 50 μm).

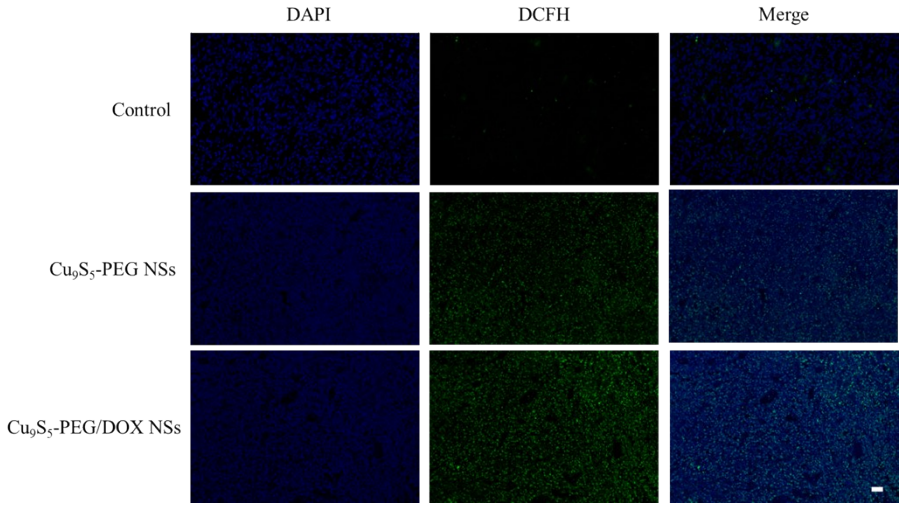

Fig. S25 DCFH staining of tumor slices of each groups. ROS were stained with DCFH (green). The nucleus was stained with DAPI (blue) (Scale = 50 μm).